

Spin polarization of electrons tunneling from 3d ferromagnetic metals and alloys

D. Paraskevopoulos,* R. Meservey, and P. M. Tedrow

Francis Bitter National Magnet Laboratory,† Massachusetts Institute of Technology, Cambridge, Massachusetts 02139

(Received 3 May 1977)

The electron spin polarization (ESP) of a wide range of alloys of Cr, Cu, Fe, Mn, or Ti in Ni was measured by the spin-polarized tunneling technique using thin-film Al-Al₂O₃-ferromagnetic-alloy tunnel junctions. The measurements were made at a temperature of 0.4 K and in an applied magnetic field of 3.5–4.0 T. A phenomenological correlation between electron spin polarization and atomic magnetic moment which was previously observed for the pure ferromagnetic elements (Fe, Co, Ni), is shown to be valid for all the alloys measured. Various methods were used for the deposition of the thin-film alloys. Each of these methods gave the same relative values of ESP when compared to Ni deposited by the same method. The dependence of the measured polarization on deposition parameters of the ferromagnetic films is presented. The effect of the properties of the superconducting aluminum films and other sources of systematic error are analyzed. The present results greatly constrain possible explanations of spin-polarized tunneling currents from 3d ferromagnetic metals based on current theories of itinerant ferromagnetism.

I. INTRODUCTION

The spin polarization of electrons emitted from 3d ferromagnetic metals has been measured recently by several different methods. The comparison of the different experimental results and their theoretical interpretation have provoked much controversy. A surprising result was that the electron tunneling measurements and the original photoemission measurements failed to reveal the large, negative electron spin polarization (ESP) that one might expect from the Stoner-Wohlfarth-Slater (SWS) theory of ferromagnetism. These results, which gave a positive ESP (electron spin predominantly in the majority direction in the ferromagnet), raised the question of whether revision was needed in the band theory of ferromagnetism or alternatively in the understanding of the photoemission and tunneling processes.

The existence of ESP was first successfully demonstrated in Gd, Dy, and Eu compounds.^{1–4} Shortly thereafter the spin polarization of photoemitted electrons was measured in Ni,⁵ and later in Co and Fe.⁶ Spin polarization of field emitted electrons was observed for EuS-coated tungsten tips.⁷ Earlier attempts to observe ESP in the 3d metals apparently had failed because of technical difficulties in the electron optics. Shortly after the photoemission experiments on Ni, the same sign and magnitude of spin polarization were obtained from a tunneling measurement.⁸ The tunneling technique was then extended to Co, Fe, and Gd,⁹ and in each case agreed rather well with the photoemission results. The results of the photoemission experiments also implied that ESP was only slightly energy dependent in the region from

E_F to $E_F - 0.8$ eV. However, recent photoemission studies by Eib and Alvarado¹⁰ report a very rapid decrease of spin polarization for energies very close to E_F .

A review of experimental work on the emission of spin-polarized electrons from 3d materials by Siegmann¹¹ has presented a strong case for the inadequacy of the SWS theory of ferromagnetism. On the other hand, the great difficulty of improving this theory has been described by Gutzwiller.¹² It has even been proposed that band splitting may not even exist in ferromagnetic nickel.¹³ Experimental techniques that have been used or proposed for measuring ESP were reviewed by Meservey, Paraskevopoulos, and Tedrow.¹⁴ In this review, results are given for the various techniques, and attempted theoretical explanations are also listed.

The purpose of the present research was to extend the experiments of spin-polarized tunneling from elemental 3d ferromagnets to various alloy 3d systems. Such an extension of experimental data should be valuable in evaluating theoretical explanations of the electron spin polarization of tunneling currents and photoemission. Earlier experiments^{9,15} showed a phenomenological correlation between polarization and atomic magnetic moment, and one would like to know whether such an effect is also valid with various ferromagnetic alloys. In addition there was a conjecture that the ESP might be associated with preferential impurity scattering of one spin direction over the other within the ferromagnet. Since the tunneling electrons presumably also carry the transport current it was thought that there might be a close correlation between the two-current theories of ferromagnetic conduction in alloys^{16,17} and the ESP. Experimental results are presented for

alloys of Ni with Cr, Cu, Fe, Mn, or Ti. A short description of some of these results has already been published.¹⁸

II. THEORY

A. Phenomenological analysis of the conductance measurements

For a spin-paired superconductor with no spin-orbit effects, there is Zeeman splitting of the quasiparticle states in an applied magnetic field.¹⁹ The BCS density of states is split into a spin-up part and a spin-down part separated in energy by $2\mu H$. The phenomenological theory of the superconductor-ferromagnetic-metal tunneling has been developed in detail earlier.⁹

The tunneling conductance of a superconductor-ferromagnetic-metal junction is obtained by calculating separately the tunneling conductance of each spin direction and assuming a parameter α which accounts for the different tunneling probability for the spin-up and spin-down electrons. α is defined as the fraction of the tunneling electrons with magnetic moment in the direction of the magnetic field (corresponding to the majority electrons in a ferromagnet), or

$$\alpha \equiv n_{\uparrow} / (n_{\uparrow} + n_{\downarrow}). \quad (1)$$

It follows that the electron spin polarization of the tunneling electrons can be defined as

$$\alpha = \frac{\sigma(+\Delta + \mu H) - \sigma(-\Delta + \mu H)}{\sigma(+\Delta + \mu H) - \sigma(-\Delta + \mu H) + \sigma(-\Delta - \mu H) - \sigma(+\Delta - \mu H)}, \quad (4)$$

where the four different values of σ correspond to the four conductance peaks in Fig. 1. To be more precise, $\sigma(-\Delta - \mu H)$ is the conductance at bias voltage V_1 , $\sigma(-\Delta + \mu H)$ at voltage V_2 , $\sigma(+\Delta - \mu H)$ at V_3 , and $\sigma(+\Delta + \mu H)$ at V_4 . We can write

$$\sigma(+\Delta - \mu H) - \sigma(-\Delta + \mu H) = \delta_1, \quad (5)$$

$$\sigma(-\Delta - \mu H) - \sigma(+\Delta + \mu H) = \delta_2, \quad (6)$$

$$\sigma(+\Delta + \mu H) - \sigma(-\Delta + \mu H) = D, \quad (7)$$

and

$$\delta_1 - \delta_2 = \delta. \quad (8)$$

Combining Eqs. (3)–(8) we obtain

$$P = \delta / (2D - \delta). \quad (9)$$

Thus, by measuring the lengths $\delta_1 - \delta_2 = \delta$ and D on a measured conductance curve, the polarization of the ferromagnetic film is obtained through Eq. (9).

$$P \equiv (n_{\uparrow} - n_{\downarrow}) / (n_{\uparrow} + n_{\downarrow}) = 2\alpha - 1. \quad (2)$$

Complete analysis of the conductance curves for the case of zero spin-orbit scattering is given in Ref. 9. It was derived analytically that the fraction α of tunneling electrons with magnetic moment in the direction of magnetic field is

$$\alpha = \frac{\sigma_4 - \sigma_2}{\sigma_4 - \sigma_2 + \sigma_1 - \sigma_3}, \quad (3)$$

where σ_1 and σ_4 are the conductances at voltages V and $-V$, respectively, (where V is any voltage), and σ_2 and σ_3 are the conductances at $V + 2\mu H$ and $-V - 2\mu H$. This result implies that any arbitrary bias voltage and applied magnetic field may be selected to determine P . However, practical limitations exist; very low values of H do not eliminate the fringing field of the ferromagnet, which causes depairing in the Al, and high values of H , close to the Al critical field, broaden the curves again due to depairing, and obscure the effect of the splitting. On the other hand, selecting arbitrarily the voltage V may introduce random errors due to high slopes of the curves, except when such selection is made so that the σ 's are close to local maxima of the conductance curve where the absolute value of the slope is small. The optimum choice of voltage is approximately $V = -\Delta - \mu H$, yielding

B. Correction due to spin-orbit scattering

When spin-orbit scattering is present in the superconductor, the density of states is unchanged at $H = 0$, but in a magnetic field the density of states is split, and states in the two-spin directions are partially mixed. This effect can be described in terms of the spin-orbit scattering parameter, defined as

$$b \equiv \hbar / 3\tau_{so} \Delta, \quad (10)$$

where τ_{so} is the spin-orbit scattering time. Engler and Fulde²⁰ have calculated the density of states in a magnetic field $\mu H / \Delta = 0.6$ for four values of b . The main feature of this result is that for small values of b , some of the spin states which comprise the peak at large values of energy are shifted by the spin-orbit interaction to near the peak at low energy. For larger values of b , this mixing of the spin states increases and the splitting of the peaks decreases until, for $b \rightarrow \infty$, the spin states

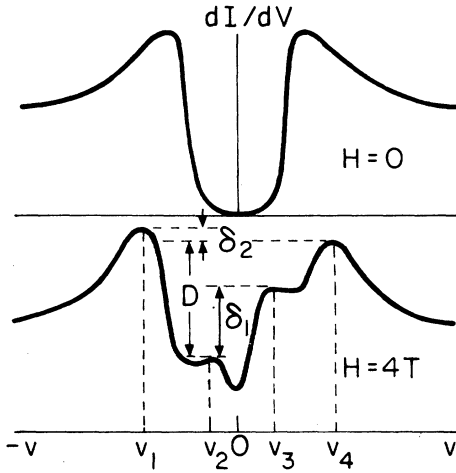


FIG. 1. Upper figure shows the tunneling conductance as a function of voltage for an Al-Al₂O₃-ferromagnetic-metal tunnel junction at $H=0$. Lower figure shows the tunnel conductance with $H=4.0$ T. The relative heights of the Zeeman split peaks at V_1 , V_2 , V_3 , and V_4 can be used to obtain the spin polarization P of the tunneling current. The value $P = (\delta_1 - \delta_2) / [D - (\delta_1 - \delta_2)]$ assumes complete spin pairing in the superconductor and is subject to correction for spin-orbit scattering. $V = V_{Al} - V_{FM}$.

are completely mixed and the two spin densities of states collapse into a single one, identical to that of the BCS theory. Bruno and Schwartz^{21,22} have calculated the density of spin states for various values of magnetic field and spin-orbit scattering, as well as the effect of spin-flip scattering caused by magnetic impurities in the superconductor. Their theoretical calculations for spin-orbit scattering were compared with experimental results²³ in Al-Al₂O₃-Ag tunnel junctions and show good agreement.

We have calculated numerically²⁴ the dynamic conductance of a superconductor-ferromagnet junction for various values of the polarization in the ferromagnet, spin-orbit scattering in the superconductor, and the depairing effect of the magnetic field on the superconductor. The apparent (measured) polarization was found from these computer results using Eq. (9). In Fig. 2, the true polarization (the one assumed for the numerical calculation) is shown as a function of the apparent polarization ignoring spin-orbit and magnetic-field depairing. The apparent polarization was always found to be greater than the true polarization. Furthermore, it can be shown analytically²⁴ that for a given value of b and orbital depairing the true polarization is a certain percent of the apparent polarization *independent* of the magnitude of the polarization. Thus the ratios of polarizations be-

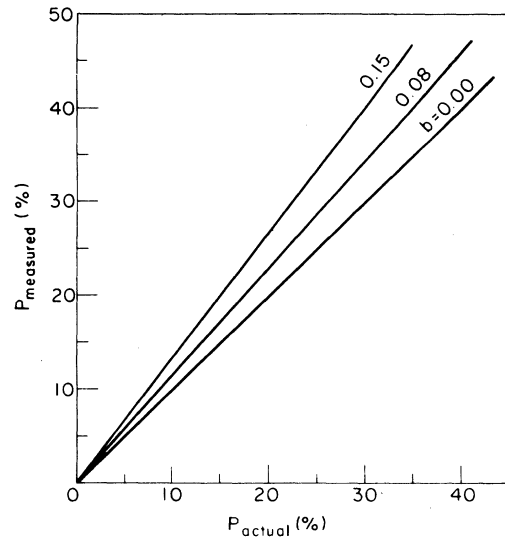


FIG. 2. Apparent (measured) polarization as a function of actual polarization for various values of spin-orbit parameter b .

tween different alloy films will be unaffected by corrections due to the spin-orbit scattering and orbital depairing.

It was previously found²³ that the parameter b for Al films similar to those used in this experiment is usually not larger than 0.08. A search for a possible correlation between the resistance per square R_s of the normal thin Al film and the Ni polarization (since b might be expected to be proportional to R_s ,²⁵ at least for large values of b) gave negative results. The Ni polarization was independent of R_s , suggesting a low value of b for our samples. A value near 0.05 gave self-consistent results for some of the most carefully measured junctions, but a highly accurate value of b is still not available.

III. EXPERIMENTAL TECHNIQUES

A. Junction preparation

The tunnel junctions were made in a conventional way. First, an Al film approximately 40 Å thick was evaporated through a mask onto a glass substrate cooled with liquid nitrogen. The pressure during evaporation was less than 10^{-6} Torr. The thickness was determined with a digital quartz crystal monitor calibrated by multiple-beam interferometer measurements. The Al film had a width of about 0.2 mm. After evaporation, the Al film was allowed to oxidize for about 10 min in room temperature air saturated with water vapor and then dried out with dust-free air for 10 min. After oxidation of the Al, the ferromagnetic metal was deposited to make a crossed junc-

tion. These cross strips had a width of 0.18 mm, yielding a junction area of $3.6 \times 10^{-2} \text{ mm}^2$. Junctions made in this way normally had an impedance of 50–500 Ω and were most satisfactory for the active four-terminal circuit arrangement described later. For two-terminal measurements, the junction impedance could be increased up to 5 k Ω by longer oxidation, thus making the thin film lead resistances negligible. The ferromagnetic films were deposited by various methods described below, but were always made 500–1000 \AA thick. Solder terminals at the ends of the metal strips were evaporated through another mask. The solder terminals consisted of a 100- \AA -thick adherence layer of Cr and a thick layer of indium-tin solder. Brass wires were soldered to the terminals. Each sample consisted of eight junctions, all having the same Al bottom film, but four of the top films were deposited with one mask and were made of the ferromagnetic alloy being studied, and the other four films were made of Ni through a second mask. In this way all measurements could be compared to the Ni junctions for reference, and effects due to variations in the properties of the Al thin films could be minimized. Thirty-two junctions were made each time, but only the eight with the most consistent impedance values in the proper range were measured and analyzed.

B. Ferromagnetic alloy deposition and composition

Three different methods were used to deposit the ferromagnetic alloy films. For alloys such as Ni-Fe and Ni-Cr for which the separate elements have nearly the same vapor pressure at the evaporation temperature the single crucible evaporation method could be used. For these substances the behavior is close to that of an ideal solution so that the deposited films had a composition close to that of the liquid evaporant. In addition, since the activity coefficients of these substances are known,²⁶ corrections can be made for the behavior of the real solutions, and the composition of the deposited films can be accurately calculated. It should be emphasized here that it is the alloy composition at the junction interface that matters, since the polarization of only the first few layers is determined by tunneling. This was demonstrated by Tedrow and Meservey²⁷ by finding that the characteristic escape length for spin polarized electrons in Co films is about 3 \AA .

For alloys of Ni with Cu, Cr, Mn, or Ti, in which the impurity element has a vapor pressure markedly different from that of Ni, simultaneous evaporation from two separate sources could be used. In the above cases Ni was evaporated by an electron gun and the impurity element from

a resistively heated tungsten boat. The use of two quartz crystal-oscillator thickness gauges provided a record of the combined mass deposited from the two sources and the mass of the deposited impurity as a function of time. When the deposition rates from the two sources had been adjusted and were steady the shutter was opened to deposit the film. The composition of the film and its homogeneity could be determined from the thickness gauge recordings.

Flash evaporation was also tried for some of the alloys. In this process a uniform mixture of fine powder of the two elements in the proper proportion is fed onto a hot tungsten surface. Since the powder is fed slowly onto the tungsten surface and all evaporates, the film is constrained in the ideal case to have the same composition as the powder mixture. In practice, there are two difficulties with this method. First, during the flash evaporation, the powder outgasses causing poor vacuum conditions which probably contaminate the film. Films made using this method showed a decrease of polarization, which probably is caused by the presence of disorder and oxides in the films. A second difficulty is caused by the streaming gas from the almost explosive evaporation which sometimes deflected very fine powders from ever reaching the hot filament. Such an effect could act differentially on the two species of powders and cause concentration errors. For these reasons the flash evaporation method was not used extensively.

To verify the accuracy of the above concentration calculations, the atomic concentration of the thin films was measured by x-ray fluorescence analysis in a scanning electron microscope. In this method, the probing electron beam penetrates to a depth of about 10 000 \AA , and therefore in passing through a film of up to 1000 \AA it is not attenuated significantly. Thus, there is little error caused by the attenuation of the electron beam or by the absorption of the emitted x-rays, but obviously the result will depend on the composition averaged over the film thickness. The atomic fraction of the minor constituent of the alloy was accurate to between about 2% and 10% depending on the situation, and the uncertainty is indicated on the data presented.

C. Measuring apparatus

The experiment was performed by measuring the normalized conductance $\sigma \equiv (dI/dV)_S / (dI/dV)_N$ as a function of voltage for the Al-Al₂O₃-Ni alloy in magnetic fields up to 4 T. The 40- \AA -thick Al films had transition temperatures close to 2.5 K and critical fields of about 5 T. The measurements

were taken at a temperature of 0.45 K, in a non-recirculating ^3He refrigerator. The magnetic field was produced either by a 2-in. bore radial-access water-cooled solenoid or a 1.5-in. axial-access superconducting coil, usually operated in the persistent mode. The superconducting coil was tipped about 5° from the vertical axis of the ^3He cryostat. As long as the junction surface was tipped less than 5° from the solenoid axis, appropriate rotation of the ^3He cryostat could always achieve parallel alignment of the field and the junction surface. However, in practice because of mutual constraints of the Dewar systems, this alignment sometimes gave a small perpendicular field which caused some depairing of the Al film. The effect of this misalignment will be discussed later. With the water-cooled radial-access solenoid exact alignment was easily attained, but the noise level was higher.

The dynamic conductance was measured by one or both of two circuits. For measurements of high-impedance junctions a two-terminal passive circuit was used. In this circuit a small constant ac voltage (usually $20\ \mu\text{V}$) was superimposed on a variable dc bias, and the synchronous change in current through the junction was measured by detecting with a lock-in amplifier the ac voltage on a series resistance R_s . Accurate operation of this circuit requires that $R_s + r_1 + r_2 \ll dV/dI \equiv R_j$ where r_1 and r_2 are the series lead resistances (including the thin film resistances). However, because the thin-film leads have considerable resistance, one may not be able to satisfy this inequality. The junction could be prepared with a high R_j , but this procedure increases the noise since the ac voltage applied to the junction is limited to $\sim k_B T/e$. The best solution was a compromise in which the nonlinear error caused by the series resistances was kept less than 3% and the circuit was calibrated with an external resistance box. In this way, the true dynamic conductance of the junction could be measured. The two terminal circuit was particularly useful for values of $R_j \geq 3\ \text{k}\Omega$.

To avoid this somewhat long and sometimes inaccurate procedure due to lack of the exact knowledge of the lead resistance, a more sophisticated circuit was built similar to that described by Hebard and Shumate.²⁸ This four-terminal dI/dV circuit is based on the same principle as the two-terminal one, but has the advantageous feature that the ac modulation level on the junction is measured by a second lock-in amplifier, compared to a reference level, and kept constant through a feedback system utilizing a multiplier. This circuit allowed accurate measurements of junctions with a normal state resistance as low as $10\ \Omega$.

However, the feedback circuit had only a limited operating range between a low resistance limit at which the response became nonlinear and a high resistance limit where the circuit became unstable. In high magnetic-field measurement, the instability level was always below the lowest point of the dI/dV curve. But, when the zero-field characteristic was traced, the bottom 10% was chopped off. For this reason, all junctions were usually measured at $H=0$ also with the two-terminal circuit, which is accurate for large values of R_j , and the accurate segments of each curve were matched to each other.

D. Measurement procedure and errors

All samples were first tested at room temperature by measuring the junction resistance by a simple four-terminal dc circuit. Then the Al and alloy thin-film strips were measured. The same procedure was repeated at a temperature of about 3 K. In this way, the resistances of the leads and junctions were found as well as their change from 300 to 3 K. The junction resistance increased by an average factor of 1.3. The higher impedance junctions increased by 1.3 to 1.5 and the lower ones by 1.1 to 1.3. Since this ratio in a normal tunnel junction should be a function only of the oxide thickness, the barrier height, and the two temperatures, the consistency of the ratios implies that all junctions measured were similar and their oxide barrier was uniform, and that none of the junctions was dominated by nontunneling spurious conductance mechanisms.

Next, the resistance of the Al strip was recorded as a function of temperature from 3 to 0.45 K. In this way the superconducting transition temperature of the thin film was determined as well as any spurious residual resistance at the lowest temperature. Subsequently, the conductance-versus-voltage curve was taken at zero field. In most cases, the fringing field of the incompletely saturated ferromagnetic film acted to change the density of states of the Al, causing some "washing-out" of the curve. Figure 3 is a graphically smoothed tracing of a set of conductance curves for a Ni junction showing a polarization of 7.64% at zero external field, at $H=0.44\ \text{T}$ which eliminates the fringing field, and at $H=3.4\ \text{T}$.

Then the conductance σ in a high magnetic field was measured as a function of voltage V on a normal calibrated scale (including the point $\sigma=0$), so that corrections due to electronic circuit nonlinearity could be calculated if necessary. Finally, the part of the σ -versus- V curve which included the four peaks and therefore the lengths δ_1 , δ_2 , and D (referring to Fig. 1) was expanded

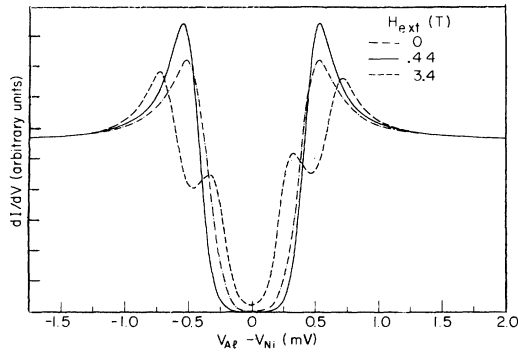


FIG. 3. Typical conductance characteristic of a pure-Ni sample made by flash evaporation and measured at $H = 0$, 0.44, and 3.4 T. Note the depaired curve at $H = 0$ due to the fringing field from the ferromagnet. At $H = 0.44$ T the magnetic domains are aligned and the depairing effect of the fringing field on the thin superconductor is minimized.

and traced on the x - y recorder three or four times. In this way, an average value of polarization of a particular alloy as well as the polarization of the Ni films sharing the same Al counter-electrode was determined, as described in Sec. IIA. About 200 junctions were measured for this work. Photoreductions of typical actual tracings for two junctions are shown. Figure 4 is the conductance curve at a high magnetic field of a Ni-Cr alloy junction showing a low polarization of 0.52%; the resistance calibration is shown as well as the resultant linear conductance. Figure 5 is the conductance curve of the same junction expanded and traced four times. Similarly, Figs. 6 and 7 are the conductance curves of Fe-Ni alloy junction showing a polarization of 46.4%.

One can refer back to Eq. (9) and Fig. 1 and assume that there is a random error ϵ of the measured conductance due to electronic noise and

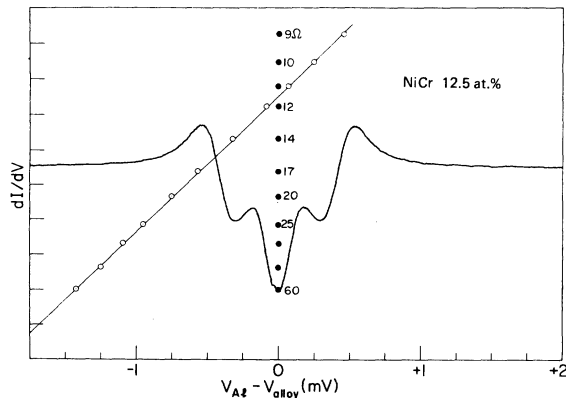


FIG. 4. Photoreduced actual tracing of the conductance curve of a Ni-Cr junction at high magnetic field.

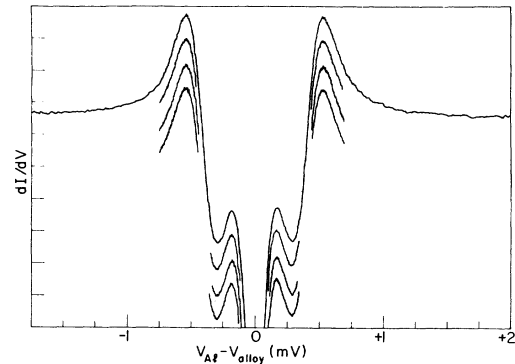


FIG. 5. Expanded conductance characteristic of the same junction as in Fig. 4.

drift. In the practical case where $D \gg \frac{1}{4}\delta$ it can be shown that the absolute error δP in the measured polarization can be approximated by

$$\delta P = \pm \epsilon/D. \quad (11)$$

The quantity D depends only on the magnitude of the conductance characteristic, and was for all measurements approximately the same and equal to 60 divisions. The error ϵ was found to be 0.5–1 divisions, dependent on the particular junction. Therefore $\delta P \approx 1\%$ and does not depend on the magnitude of the polarization. Since four or five curves were taken for each junction the average result had a random error of about 0.5% absolute polarization.

It was shown experimentally^{8,9} that the electron spin polarization is independent of the parallel magnetic field, as long as this is not close to the critical field of the thin Al film. The experimental curves were also fitted to theoretical calculations,²³ and it was shown that P does not depend on the depairing parameter associated with the

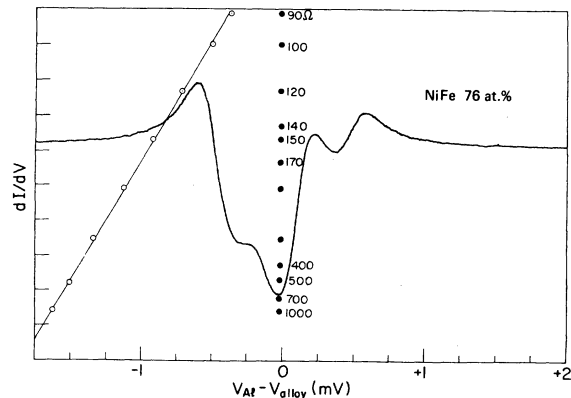


FIG. 6. Photoreduced actual tracing of a Ni-Fe junction at high magnetic field.

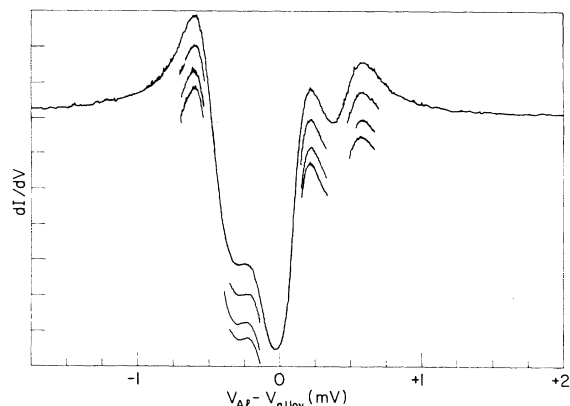


FIG. 7. Expanded conductance characteristic for the same junction as in Fig. 6.

parallel magnetic field.

As mentioned in Sec. IIC, the film could, in principle, be exactly aligned with the magnetic field by rotating the liquid ^3He Dewar about its symmetry axis which was in the vertical direction. Since the plane of the film was very nearly parallel to the vertical axis and the axis of the solenoid was tipped at about 5° from the vertical, when the Dewar was rotated 360° there should be two positions in which the magnetic field is exactly parallel to the plane of the film. However, the constraint of the solenoid on the flexible Dewar sometimes prevented a perfect alignment and caused some additional depairing in the Al film from a small perpendicular field. This effect could not be corrected for because it was discovered near the end of the measurement series. However, by applying a known perpendicular field we could determine the effect of this additional depairing on P . The apparent value of P was always diminished by the perpendicular field. The largest possible absolute error from this cause was about the same as or less than other sources of error. Since the effect was linear over the region of interest, relative values of P were unaffected.

IV. EXPERIMENTAL RESULTS

First, Fe-Ni alloys were measured. They were prepared by the single crucible method described in Sec. IIIB. In Fig. 8 the measured polarization of various alloy compositions (circles) is plotted versus the corresponding magnetic moment for bulk alloys. The straight line is a least-squares fit of the Fe-Ni alloy data only, assuming a linear relation between P and n_B , where n_B is the atomic magnetic moment in Bohr magnetons. The squares are the earlier results¹⁵ for the three pure elements Fe, Co, and Ni which are superimposed

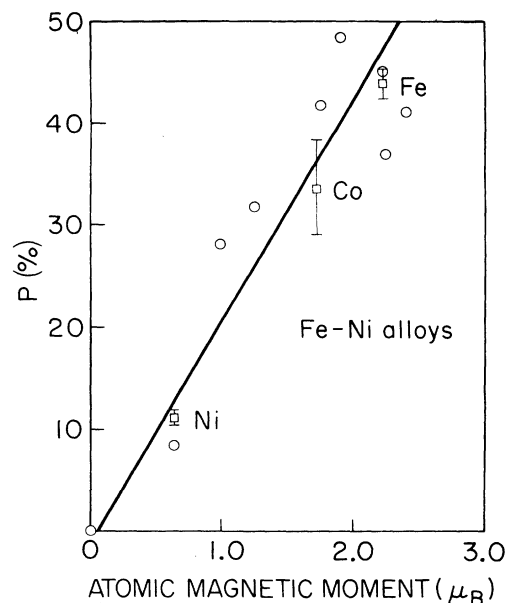


FIG. 8. Measured polarization of Fe-Ni alloys (circles) as a function of atomic magnetic moment. The straight line is a least-squares fit of the alloy data. The squares are earlier results for the three pure elements.

on the diagram to show that the proportionality constant P/n_B is, within the experimental errors, the same for the alloy and the pure ferromagnetic films, and approximately equal to 0.2. If for the moment we assume that the polarization is accurately proportional to the magnetic moment, the scatter in the results is larger than the random measuring errors. Part of this scatter may be attributed to the use of the bulk value of magnetic moments for the alloys whereas the magnetic moments of the thin films were presumably affected by inhomogeneity, disorder, impurities, and stresses in the films.

For this reason, we plot the above data in a different way shown in Fig. 9. Both the polariza-

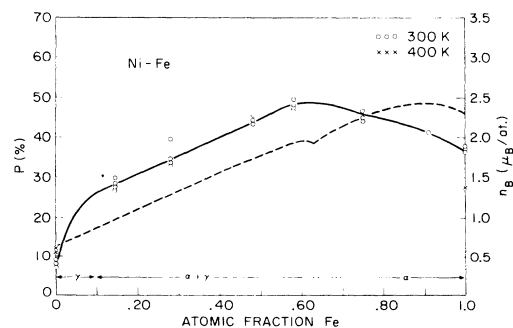


FIG. 9. Polarization measurements and atomic magnetic moments (dashed line) of Fe-Ni alloys as a function of Fe concentration. The substrate temperature is shown.

tion P and atomic moment n_B of bulk alloys are plotted versus the alloy composition. The dashed line corresponds to n_B at absolute zero and is taken from the literature.²⁹ The circles are the measured values of P . It is clear that the spread in the data is rather small, and that the dashed and solid lines do not have the same shape. However, in the composition range of about (10–60) at.% Fe, both P and n_B are proportional to the concentration. In this range, Fe and Ni form a continuous series of solid solutions,³⁰ and the magnetic anisotropy constant K_1 is close to zero for both crystalline³¹ and polycrystalline alloys.³² Above and below this range K_1 becomes large. It is not obvious at this point what role K_1 plays in the alloy structure and polarization. However, when the substrate temperature is raised to 400 K prior to deposition of the film, the resultant values of the pure-Ni polarization are increased as shown by the α 's at 100% Ni in Fig. 9. This finding is consistent with the photoemission results. High substrate temperature is known to yield Ni films with lower K_1 (Ref. 33) and high magnetic moment, as well as decreased stresses. On the other hand, the decrease of the Fe polarization with increased substrate temperature might be attributed to some effect between the first few layers of deposited Fe and Al_2O_3 , accompanied by a drastic decrease in the tunnel junction resistance.

Dilute alloys of Mn, Ti, Cu, or Cr in Ni were also measured and the results are shown in Figs. 10–13. All three deposition methods described in Sec. IIIB were used to form the alloys. In these figures the circles represent alloys prepared by separate source coevaporation, the triangles by flash evaporation, and the squares by the single crucible method. Different methods were usually

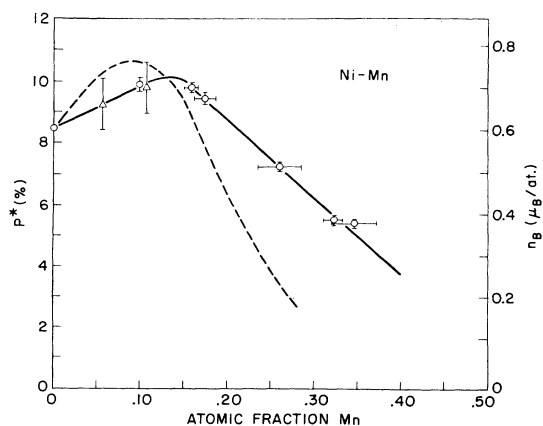


FIG. 10. Normalized polarization measurements and atomic magnetic moments (dashed line) of Ni-Mn alloys as a function of Mn concentration.

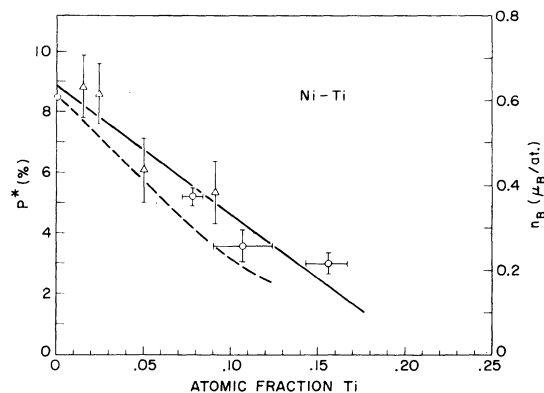


FIG. 11. Normalized polarization measurements and atomic magnetic moments (dashed line) of Ni-Ti alloys as a function of Ti concentration.

tried to determine which was most practical for a given alloy. For Ni-Mn where the two elements have very different vapor pressures, the single-source method was not used. Although flash evaporation seemed to be the most straightforward method of preparation of any alloy, the outgassing of the powders always decreased the polarization as compared to the other two methods. In the case of Ni-Cr flash evaporation was not tried because the Cr was in the form of small slugs. In Figs. 10–13 we plot the normalized polarization $P^* = (P_{\text{alloy}}/P_{\text{Ni}})\langle P_{\text{Ni}} \rangle$ which is proportional to the ratio of the measured values of P for the alloy and for pure Ni prepared during the same evaporation. $\langle P_{\text{Ni}} \rangle$ is the value of P for pure Ni averaged over many evaporations. This normalization procedure is very useful for alloys with low concentrations of the element alloyed with Ni and low polarizations. Absolute changes in P caused by variations in film preparation method tend to be eliminated, as well as the effect of spin-orbit scattering and magnetic field depairing

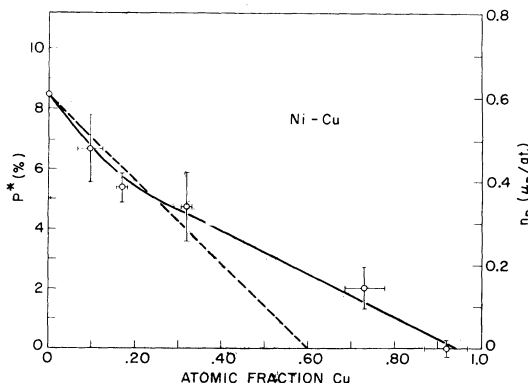


FIG. 12. Normalized polarization measurements and atomic magnetic moments (dashed line) of Ni-Cu alloys as a function of Cu concentration.

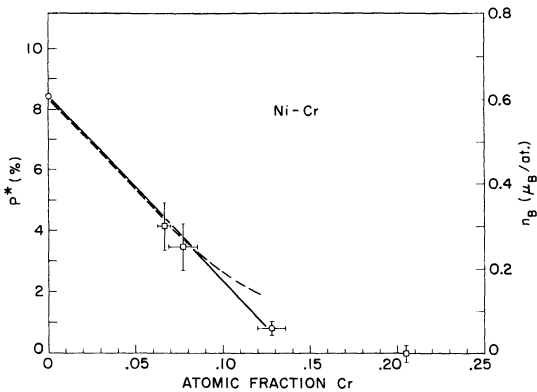


FIG. 13. Normalized polarization measurements and atomic magnetic moments (dashed line) of Ni-Cr alloys as a function of Cr concentration.

on the superconducting film as discussed above. In measurements of Ni-Fe alloys where the values of P are relatively large compared to variation among samples, this normalization procedure is unnecessary. The dashed lines are the magnetization versus concentration results taken from the literature.³⁴ The solid lines in Figs. 11 and 13 are least-squares fits of the data assuming a linear relationship between P and n_B . The ones in Figs. 10 and 12 are simply drawn through the data points. The error bars are estimated in the following way: one standard deviation of the polarization in both Ni and alloy is calculated from the data; the relative errors of the two are added, and the result multiplied by $\langle P_{Ni} \rangle$. The concentration values are the average of the calculated values and those measured by x-ray fluorescence, and the error bar is the difference of the two. There is one more experimental point not shown in the Ni-Mn curve, corresponding to about 88 at.% Mn and giving a polarization of 1.25%. It is expected that the polarization would have dropped to about zero at such a composition, and it is probable that at such a high Mn content the films are inhomogeneous having different regions rich in either Mn or Ni, the latter ones causing this slight polarization.

Certain deposition parameters were varied to study their possible effects on polarization. The results of Ni measurements are shown in Fig. 14. The data are grouped by the method of evaporation. Each point represents one sample, i.e., one to four junctions where the value for each junction is the average of three to four measurements. The dashed lines represent the average polarization for each subgroup. The most consistent results are those for films evaporated from a tungsten boat; the polarization was increased for a substrate temperature of 400 K and decreased for a substrate temperature of 100 K in agreement with the photoemission re-

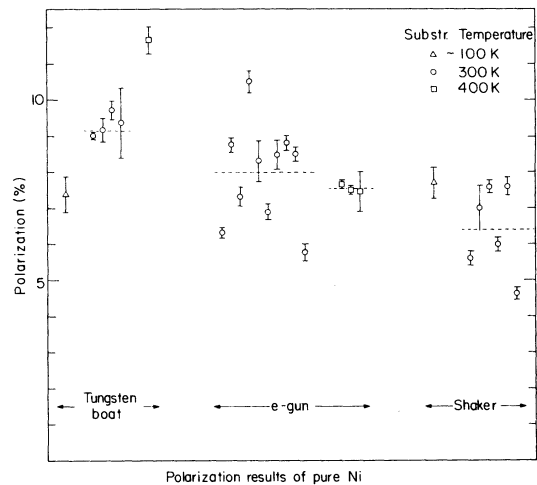


FIG. 14. Pure Ni sample polarizations for various deposition parameters.

sults. In the e -gun group the scatter was larger, the average polarization somewhat lower, and there is no significant effect from heating the substrate. The average polarization of the Ni films made by flash evaporation was considerably lowered, and there was no significant effect from cooling the substrate. As mentioned before, it is believed that the reduced polarization of films made by flash evaporation was due to outgassing of the powder causing disorder in the films. Also, Fe deposited by flash evaporation had a polarization which was decreased to about 34%. To test this assumption, a sample was prepared with four junctions made from powder by flash evaporation and the other four junctions made from small pieces of thin Ni foil also by flash evaporation. It was expected that the one order of magnitude higher volume to surface ratio for the foil should lead to much less outgassing. The powder gave $P = (5.61 \pm 0.2)\%$ whereas the foil gave $P = (6.35 \pm 0.1)\%$, which are consistent with the above hypothesis.

The reason for the considerable scatter of the Ni data in Fig. 14 is not clear at this point. Apparently some evaporation parameter which affected the absolute polarization of both the alloy and the pure Ni films was not being adequately controlled. It is believed that one factor responsible for the scatter is the depairing effect on the superconducting Al, as described in Sec. III D, but the extent of this effect is not known. However, even in the worst case this could only explain at most half of the scatter.

It was mentioned earlier that the fringing magnetic field of the ferromagnetic alloy causes a field perpendicular to the thin Al film at zero applied field, resulting in depairing of the Al and some "washing out" of the conductance character-

istic, but when a small parallel external field was applied, the curves sharpened as shown in Fig. 3. The height of the highest conductance peak was measured as a function of applied field for a number of different alloys. It always showed an increase with field, a saturation, and a slow decrease caused by the splitting of the peak and the depairing due to the parallel field. The saturation is believed to occur when the applied field aligns the magnetic domains in the ferromagnetic films and minimizes the fringing field associated with domain flux closure outside the film. The saturation threshold field H_t was measured and found to depend on alloy composition and deposition method. For pure Ni the results are summarized in Table I. Apparently there is no significant difference between the e -gun and the tungsten boat but flash evaporation causes an increased H_t . Again, it is reasonable to assume that this is explained by the increased disorder caused by the relatively poor vacuum conditions during the flash evaporation of the powder, and it is consistent with the intermediate value of H_t obtained when pieces of foil were used with the shaker. All Fe-Ni alloys with composition of over 20 at.% Fe had $H_t = 0$. The other alloys showed an initial increase in H_t vs impurity concentration and a decrease at higher concentrations, with $H_t \rightarrow 0$ as the polarization tended to zero. Substrate temperature (400 to 100 K) did not affect H_t significantly.

V. DISCUSSION

The band structure of ferromagnetic Ni has been extensively studied,^{35,36} and the density of states can be calculated on the basis of the Stoner-Wohlfarth-Slater theory. According to this view, the majority-spin d -electron band is completely filled, its top being below E_F . At E_F the density of minority-spin states predominates. Thus, it was expected that photoemission from close to E_F would give negative (that is, minority) electron spin polarization and that positive polarization would be observed at energies further below E_F . Actually, in the original experiments on films,^{5,6} a positive polarization was measured which varied little with energy in the region 0.4 to 0.8 eV below E_F . A recent result by Eib and Alvarado¹⁹ of

photoemitted electrons from Ni (100) and (111) single-crystal surfaces shows a sudden decrease in the polarization near E_F and gives negative polarization for energies less than 0.05 eV below E_F . These latest results depend sensitively on the work function of the surface, which changes as much as 0.10 eV during a measurement, so that the interpretation may be complicated by threshold effects.

Wohlfarth³⁷ has shown that the earlier photoemission results in Ni do not necessarily conflict with the SWS theory with plausible values of the band splitting and the energy gap between the top of the d band and E_F . Furthermore, as Wohlfarth³⁸ has recently pointed out, the latest experimental results are in good agreement with his original calculation of the energy dependence of the polarization in Ni. However, when such a model is applied to the density of states of Co or Fe,³⁹ the results appear to disagree with experiment. Smith and Traum⁴⁰ have assumed momentum conservation in the photoemission process and calculated a complicated dependence of the sign and magnitude of P on the initial electron energy and the photon energy. This view appears to conflict with the very simple dependence of P on photon and electron energies obtained in cesium-coated nickel.⁴¹ Magneto-optical Kerr effect (MOKE) measurements in Ni appear to be consistent with the density of states of the SWS theory, although for Co and Fe the situation is more obscure.^{42,43} For Ni it should be realized that the quantity measured by MOKE is probably quite different from that measured in photoemission, field emission, or tunneling because an electron is not extracted from the metal.

A calculation of the field emission from the (100) plane of Ni by Politzer and Cutler⁴⁴ giving $P = -4\%$ agrees approximately with $P = -10\%$ obtained in field emission experiments by Gleich *et al.*⁴⁵ Field emission experiments by Landolt *et al.*⁴⁶ showed initially positive P for both Ni (100) and (110) tips but more recent results⁴⁷ indicate $P = (-3 \pm 1)\%$ for the Ni (100) plane. Since the photoelectric and tunneling results were in polycrystalline samples they do not necessarily conflict with this calculation. Previous field emission work⁴⁸⁻⁵⁰ showed that the interpretation of these experiments may be complicated, and further confirmation was needed. One conclusion of the Politzer-Cutler calculation is that the field emission in the [100] direction consists largely of electrons in the $4s-p$ band, and that the high polarization of the d band (-80%) only contributes sufficiently to give a net $P = -4\%$. This result seems to agree with x-ray measurements which show a negative polarization in the outer parts of the unit cell and with the deuteron reflection measurements which also give

TABLE I. H_t of Ni films for various deposition methods.

Source	$H_t(T)$
Tungsten boat	0.237 ± 0.045
e -gun	0.236 ± 0.053
Flash evaporation	
{ Powder	0.418 ± 0.087
{ Foil	0.36

negative polarization outside the metal surface.⁵¹

In the tunneling experiments, it was originally assumed that the electron polarization would be negative in Ni because of the high density of states in the minority direction at E_F . However, there seems to be no firm basis for such an expectation. For a simple one-dimensional band model, Harrison⁵² has shown that the density of states does not enter into the magnitude of the tunneling current. This proof certainly has a limited range of validity, but it shows that the observed positive polarization is not necessarily in conflict with band calculations. On the other hand, the agreement of tunneling and photoemission does appear to conflict with a simple interpretation of the experiments on the basis of the SWS band theory. One way to explain the tunneling results has been advanced by Fulde *et al.*⁵³ They calculated that the surface layer of ferromagnetic Ni is positively polarized. Kautz and Schwartz⁵⁴ also calculated the variations caused by a surface in the relative spin density in a spin-polarized electron gas. It is reasonable that tunneling should be determined mainly by the surface, but again the agreement with photoemission, which has a characteristic probing depth of 10 Å, makes this view difficult to maintain.

A number of attempts have been made to include many-body effects in ferromagnetic band calculations.⁵⁵⁻⁵⁹ In particular Hertz and Aoi⁵⁸ have presented a theory which applies to tunneling. They assume, on the basis of a plausible estimate and the calculation of Politzer and Cutler for Ni, that the tunneling current consists predominantly of s electrons. According to these authors s - d hybridization leads to a positive polarization which is of the proper size if spin-wave emission self-energy effects are included. The values estimated for Fe, Co, and Ni are 37%, 26%, and 8%, respectively. This theoretical picture implies that the conduction properties of the two spin directions are of primary importance in determining P . Although the estimated values of polarization are of the right sign and magnitude to agree with experiment, the question remains how to interpret the photoemission results in this picture. The "interstitial-electron" model by Johnson⁶⁰ assumes a partition of electrons into itinerant and localized d electrons and claims to have accounted for the photoelectric results.

Our experimental results show a striking consistency strongly supporting the idea that the electron spin polarization is directly proportional to the net atomic magnetic moment of the $3d$ metals, the quantitative relation being approximately $P/n_B = 0.2$. This result cannot be readily accounted for by any presently well accepted theoretical model describing ferromagnetism. It may be possible

for the Hertz and Aoi⁵⁸ model to explain these results as it did for the pure elements, but this remains to be proven. Since the basic feature of the present results is the direct relationship between electron spin polarization and atomic magnetic moment, any successful model will have to show such a generalized result. Goodenough,⁶¹ using a departure from conventional energy-band calculations, has described the dependence of the magnetic moment on impurity concentration in ferromagnetic alloys. Stearns⁶² has used a model that assumes a predominant number of localized d -like electrons indirectly coupled through a small number of itinerant d -like electrons to describe ferromagnetism. Recently she has applied this model to tunneling into Fe, Ni, and Co,⁶³ and considered the tunneling process with ferromagnets in a manner similar to Bardeen's explanation of the observation of the density of states in tunneling with superconductors. The result for the polarization P_x of a Ni alloy is

$$P_x = \frac{(E_0 + \Delta_x)^{1/2} - (E_0 - \Delta_x)^{1/2}}{(E_0 + \Delta_x)^{1/2} + (E_0 - \Delta_x)^{1/2}} \approx \frac{\Delta_x}{2E_0},$$

where E_0 is the energy (in the nonmagnetic state) below E_F of the bottom of the conduction band of the quasi-free-electrons which do the tunneling and $2\Delta_x$ is the ferromagnetic splitting of this band. It is also assumed that $2\Delta_x = U\mu_x$, where U is the exchange splitting per Bohr magneton⁶⁴ which is taken to be essentially constant for $3d$ ferromagnets. Stearns therefore concludes that $P_x/P_{Ni} = \mu_x/\mu_{Ni}$, a result which agrees generally with the present tunneling experiments. Assuming this point of view, from our experimental result of $P_x/\mu_x \approx 0.2$ and the assumption that $E_0 = 2.2$ eV we can calculate U to be 1.76 eV/ μ_B which compares favorably with previous experiments⁶⁴ that find U to be about 1.8 for Ni and Co and 1.6 for Fe.

The conjecture that the ESP might be associated with preferential impurity scattering of conduction electrons on one spin direction over the other within the ferromagnet was also examined. According to resistivity measurements in ferromagnetic alloys¹⁶ analyzed on the basis of the two-current model and data recently compiled by Dorleijn and Miedema,¹⁷ impurities of Cu should scatter minority spins preferentially and might be expected to increase the spin polarization. No such effect was observed, and the results have been discussed in a recent publication.⁶⁵

VI. CONCLUSIONS

Although comparison of tunneling results with those from photoemission, field emission, and other methods of measuring ESP is interesting,

there appears to be no present basis for believing that the results should be the same. The quantities being measured by the different techniques may be quite different. For instance, small changes in the work function caused by surface conditions are important for field emission and for threshold photoemission. For tunneling, such surface effects may be of minor importance. The presence of high electric fields is probably important in the interpretation of field emission results. With the magneto-optical Kerr effect, the fact that the electron spin is detected without removing it from the metal is probably of fundamental importance.

Concerning the present tunneling measurements we have shown that for a rather wide range of 3d ferromagnetic metals and alloys the spin polarization of tunneling electrons is approximately pro-

portional to the saturation magnetic moment. This simple and general result evidently reflects a common property of the 3d ferromagnetic metals rather than the peculiarities of any particular substance.

ACKNOWLEDGMENTS

One of us (D.P.) is grateful to Professor G. O. Zimmerman for continuous encouragement and for arranging for financial support during the course of this work. We wish to thank Dr. M. B. Stearns and Dr. M. Landolt for informing us of their results prior to publication. We also thank R. MacNabb for making the samples used in this experiment, and Michael Blaho for technical assistance.

*Part of this work was submitted in partial fulfillment of the requirements for the degree of Doctor of Philosophy at Boston University.

†Supported by the NSF.

¹G. Busch, M. Campagna, P. Cotti, and H. C. Siegmann, *Phys. Rev. Lett.* **22**, 597 (1969).

²U. Bänninger, G. Busch, M. Campagna, and H. C. Siegmann, Conference Internationale de Magnetisme, Grenoble, France, 1970 (unpublished).

³G. Busch, M. Campagna, and H. C. Siegmann, *Solid State Commun.* **7**, 775 (1969).

⁴G. Busch, M. Campagna, and H. C. Siegmann, *J. Appl. Phys.* **41**, 1044 (1970).

⁵U. Bänninger, G. Busch, M. Campagna, and H. C. Siegmann, *Phys. Rev. Lett.* **25**, 585 (1970).

⁶G. Busch, M. Campagna, and H. C. Siegmann, *Phys. Rev. B* **4**, 746 (1971).

⁷N. Müller, W. Eckstein, W. Heiland, and W. Zinn, *Phys. Rev. Lett.* **29**, 1651 (1972).

⁸P. M. Tedrow and R. Meservey, *Phys. Rev. Lett.* **26**, 192 (1971).

⁹P. M. Tedrow and R. Meservey, *Phys. Rev. B* **7**, 318 (1973).

¹⁰W. Eib and S. F. Alvarado, *Phys. Rev. Lett.* **37**, 444 (1976).

¹¹H. C. Siegmann, *Phys. Rep. C* **17**, 37 (1975).

¹²M. C. Gutzwiller, *AIP Conf. Proc.* **10**, 1197 (1973).

¹³J. Schones and P. Wachter, *Phys. Rev. B* **9**, 3097 (1974).

¹⁴R. Meservey, P. M. Tedrow, and D. Paraskevopoulos, *AIP Conf. Proc.* **29**, 276 (1976).

¹⁵R. Meservey and P. M. Tedrow, *Proceedings of the Thirteenth International Conference on Low Temperature Physics*, edited by K. D. Timmerhaus, W. J. O'Sullivan, and E. F. Hammel (Plenum, New York, 1974), Vol. 2, pp. 405-409.

¹⁶A. Fert and I. A. Campbell, *Phys. Rev. Lett.* **21**, 1190 (1968); O. Jaoul and I. A. Campbell, *J. Phys. F* **5**, L69 (1975), and references contained therein.

¹⁷J. W. F. Dorleijn and A. R. Miedema, *AIP Conf. Proc.* **34**, 50 (1976).

¹⁸R. Meservey, D. Paraskevopoulos, and P. M. Tedrow, *Phys. Rev. Lett.* **37**, 858 (1976).

¹⁹R. Meservey, P. M. Tedrow, and P. Fulde, *Phys. Rev. Lett.* **25**, 1270 (1970).

²⁰H. Engler and P. Fulde, *Z. Phys.* **247**, 1 (1971).

²¹R. Bruno and B. B. Schwartz, *Phys. Rev. B* **8**, 3161 (1973).

²²R. Bruno, Ph.D. thesis (MIT, 1972) (unpublished).

²³R. Meservey, P. M. Tedrow, and R. C. Bruno, *Phys. Rev. B* **11**, 4224 (1975).

²⁴Preliminary results were reported in D. Paraskevopoulos, R. Meservey, and P. W. Tedrow, *Bull. Am. Phys. Soc.* **21**, 341 (1976). A detailed report will be published elsewhere.

²⁵P. M. Tedrow and R. Meservey, *Phys. Rev. B* **8**, 5098 (1973).

²⁶See *Handbook of Thin Film Technology*, edited by L. I. Maissel and R. Glang (McGraw-Hill, New York, 1970), Part I.

²⁷P. M. Tedrow and R. Meservey, *Solid State Commun.* **16**, 71 (1975).

²⁸A. F. Hebard and P. W. Shumate, *Rev. Sci. Instrum.* **45**, 529 (1974).

²⁹R. M. Bozorth, *Ferromagnetism* (Van Nostrand, New York, 1951), p. 109, and references therein.

³⁰Reference 29, p. 102.

³¹Reference 29, pp. 31 and 571.

³²M. Prutton, *Thin Ferromagnetic Films* (Butterworths, Washington, D. C., 1964), p. 99.

³³Reference 32, p. 198.

³⁴The Ni-Ti data were taken from Ref. 29, p. 325. The Ni-Mn data were taken from Ref. 29, p. 440; also Tebble and D. J. Craik, *Magnetic Materials* (Wiley-Interscience, London, 1969), p. 14. The Ni-Cr data were taken from Ref. 29, p. 308; H. C. Van Elst, B. Lubach, and G. J. Van Den Berg [*Physica (Utr.)* **28**, 1297 (1962), p. 118] claim that two of their Ni-Cr alloys show magnetic moments that fall exactly on the line extending to 10 at.% Cr. The Ni-Cu data were taken from Ref. 29, p. 440.

³⁵L. Hodges, H. Ehrenreich, and N. D. Lang, *Phys. Rev.*

- 152, 505 (1966).
- ³⁶E. I. Zornberg, Phys. Rev. B 1, 244 (1970), and references given in this paper.
- ³⁷E. P. Wohlfarth, Phys. Lett. A 36, 131 (1971).
- ³⁸E. P. Wohlfarth, Phys. Rev. Lett. 38, 524 (1977).
- ³⁹E. P. Wohlfarth, J. Appl. Phys. 41 (1970); S. Wakoh and J. Yamashita, J. Phys. Soc. Jpn. 21, 1712 (1966).
- ⁴⁰N. V. Smith and M. M. Traum, Phys. Rev. Lett. 27, 1388 (1971).
- ⁴¹H. Adler, M. Campagna, and H. C. Siegmann, Phys. Rev. B 8, 2075 (1973).
- ⁴²J. L. Erskine and E. A. Stern, Phys. Rev. Lett. 30, 1329 (1973).
- ⁴³G. S. Krinchik and A. V. Artemiev, Sov. Phys.-JETP 26, 1080 (1968).
- ⁴⁴B. A. Politzer and P. H. Cutler, Phys. Rev. Lett. 28, 1330 (1972).
- ⁴⁵W. Gleich, G. Regenfus, and R. Sizmann, Phys. Rev. Lett. 27, 1066 (1971).
- ⁴⁶M. Landolt, M. Campagna, J.-N. Chazalviel, Y. Yafet, and B. B. Wilkens, J. Vac. Sci. Technol. 14, 468 (1977).
- ⁴⁷M. Landolt, M. Campagna, B. Wilkens, J.-N. Chazalviel, and Y. Yafet, Bull. Am. Phys. Soc. 22, 433 (1977); also M. Landolt and M. Campagna, Phys. Rev. Lett. 38, 663 (1977).
- ⁴⁸N. Müller, Phys. Lett. A 54, 415 (1975).
- ⁴⁹M. Campagna, T. Utsumi, and D. N. E. Buchanan, J. Vac. Sci. Technol. 13, 193 (1976).
- ⁵⁰G. Regenfus and P. Sutsch, Z. Phys. 266, 319 (1974).
- ⁵¹C. Rau and R. Sizmann, *Proceedings of the Fifth International Conference on Atomic Collisions in Solids*, edited by S. Datz (Plenum, New York, 1975), pp. 295-303; W. Brandt and R. Sizmann, Phys. Lett. A 37, 115 (1971).
- ⁵²W. A. Harrison, Phys. Rev. 123, 85 (1961).
- ⁵³P. Fulde, A. Luther, and R. E. Watson, Phys. Rev. B 8, 440 (1973).
- ⁵⁴R. L. Kautz and B. B. Schwartz, J. Magn. Magn. Mater. 1, 351 (1976).
- ⁵⁵P. W. Anderson, Philos. Mag. 24, 203 (1971).
- ⁵⁶S. Doniach, AIP Conf. Proc. 5, 549 (1972).
- ⁵⁷J. A. Hertz and D. M. Edwards, Phys. Rev. Lett. 28, 1334 (1972).
- ⁵⁸J. A. Hertz and K. Aoi, Phys. Rev. B 8, 3252 (1973).
- ⁵⁹D. J. Kim (unpublished).
- ⁶⁰O. Johnson, Solid State Commun. 14, 751 (1974).
- ⁶¹J. B. Goodenough, Phys. Rev. 120, 67 (1960).
- ⁶²M. B. Stearns, Phys. Rev. B 8, 4383 (1973).
- ⁶³M. B. Stearns, J. Magn. Magn. Mater. 5, 167 (1977).
- ⁶⁴M. B. Stearns and L. A. Feldkamp, AIP Conf. Proc. 29, 286 (1976).
- ⁶⁵R. Meservey, D. Paraskevopoulos, and P. M. Tedrow, Physica (Utr.) 91B, 91 (1977).